Inorganic Chemistry

Article

pubs.acs.org/IC

Thermally Activated Delayed Fluorescence (TADF) and Enhancing Photoluminescence Quantum Yields of [Cu^{I}(diimine)(diphosphine)]$^{+}$ Complexes—Photophysical, Structural, and Computational Studies

Charlotte L. Linfoot,[†] Markus J. Leitl,[‡] Patricia Richardson,[†] Andreas F. Rausch,[‡] Oleg Chepelin,[†] Fraser J. White,[†] Hartmut Yersin,*[,‡] and Neil Robertson*[,†]

[†]EaStCHEM School of Chemistry, University of Edinburgh, King's Buildings, Edinburgh, EH93JJ, United Kingdom

[‡]Institute for Physical und Theoretical Chemistry, University of Regensburg, Universitätsstr. 31, 93053 Regensburg, Germany

Supporting Information

ABSTRACT: The complexes [Cu(I)(POP)(dmbpy)][BF_4] (**1**) and [Cu(I)(POP)(tmbpy)][BF_4] (**2**) (dmbpy = 4,4′-dimethyl-2,2′-bipyridyl; tmbpy = 4,4′,6,6′-tetramethyl-2,2′-bipyridyl; POP = bis[2-(diphenylphosphino)-phenyl]ether) have been studied in a wide temperature range by steady-state and time-resolved emission spectroscopy in fluid solution, frozen solution, and as solid powders. Emission quantum yields of up to 74% were observed for **2** in a rigid matrix (powder), substantially higher than for **1** of around 9% under the same conditions. Importantly, it was found that the emission of **2** at ambient temperature represents a thermally activated delayed fluorescence (TADF) which renders the compound to be a good candidate for singlet harvesting in OLEDs. The role of steric constraints within the complexes, in particular their influences on the emission quantum yields, were investigated by hybrid-DFT calculations for the excited triplet state of **1** and **2** while manipulating the torsion angle between the bipyridyl and POP ligands. Both complexes showed similar flexibility within a ±10° range of the torsion angle; however, **2** appeared limited to this range, whereas **1** could be further twisted with little energy demand. It is concluded that a restricted flexibility leads to a reduction of nonradiative deactivation and thus an increase of emission quantum yield.

INTRODUCTION

Transition metal complexes are of great interest for electroluminescent devices such as organic light-emitting diodes (OLEDs),[1−6] light-emitting electrochemical cells (LEECs),[7−9] sensors,[10−12] and dye-sensitized solar cells (DSSCs).[13−27] For these applications, heavy metal complexes based on Ru(II),[28−32] Ir(III),[33−37] and Pt(II)[37−42] have been the focus of research due to their high emission quantum yields, short emission decay times, photostability, and/or tuneable emission wavelengths through intelligent ligand design. Related research into first-row transition metal complexes has been gaining momentum in the past 30 years thanks to the early work of McMillin et al.[43−47] In particular, Cu(I) compounds have attracted significant research attention recently as they provide an attractive alternative to expensive, less abundant, and more toxic heavy-metal-containing complexes. Furthermore, copper compounds can exhibit an additional radiative decay channel via thermally activated delayed fluorescence (TADF) which results in high emission quantum yields and short emission decay times.[48−51,37] More importantly, TADF emitters can utilize all injected excitons, singlets *and* triplets, for the generation of light in OLEDs resulting in a singlet state emission. The corresponding mechanism represents the singlet harvesting effect.[37,48−51] All these factors render Cu(I) compounds attractive for the use in electroluminescent devices making them replacements for heavy metal photo- and electroluminescent complexes.[15,37,48−60]

However, on excitation, Cu(I) compounds can undergo a formal oxidation of Cu(I) to Cu(II) due to the pronounced metal-to-ligand charge transfer (MLCT) character of the transition.[54−65,51,37] As a consequence, the conformational geometry can distort significantly, opening a very effective nonradiative deactivation pathway. Many literature studies have explored coordinating ligands that act to sterically constrain the pseudotetrahedral Cu(I) geometry, therefore limiting the extent of the geometrical flattening.[43−52,60−62,66−76]

In this work, we expand understanding of the structural and emissive behavior of heteroleptic Cu(I) complexes by experimental and computational investigations of bis[2-(diphenylphosphino)-phenyl]ether (POP) containing Cu(I) complexes. Prior research into [Cu(I)(POP)(diimine)]$^{+}$ complexes[77−82] has focused on 1,10-phenanthroline diimine ligands with an emission quantum yield of Φ_{PL} = 69% achieved in PMMA film.[79] Less work has been done to investigate the emission behavior of the analogous [Cu(I)(POP)(2,2′-

Received: April 15, 2014
Published: July 23, 2014

   dx.doi.org/10.1021/ic500889s | *Inorg. Chem.* 2014, 53, 10854−10861

bipyridine)]$^+$ complexes, presumably due to the typically lower quantum yields observed for Cu(I)-bipyridine complexes in comparison with the analogous phenanthrolines.[83,84,53] In a previous report, we qualitatively noted the strikingly different emissive properties of [Cu(I)(POP)(dmbpy)][BF_4] (**1**) and [Cu(I)(POP)(tmbpy)][BF_4] (**2**) (dmbpy = 4,4′-dimethyl-2,2′-bipyridyl; tmbpy = 4,4′,6,6′-tetramethyl-2,2′-bipyridyl) within a larger body of work on Cu(I) complexes.[85] We now follow this up by quantifying the photoluminescence quantum yields and excited-state lifetimes of **1** and **2** under variation of temperature in different media. The results of the measurements are interpreted through a computational density functional theory (DFT) investigation that explores in particular the link between structural rigidity and photophysical behavior. This is also facilitated by the determination of an X-ray structure of **2**. Although a general correlation between rigidity and enhanced quantum yield is well-known, investigation of more specific rigidity-property relationships has not been significantly addressed yet and may provide guidelines on the optimization of future complexes. Furthermore, a detailed analysis of the temperature dependent decay behavior of compound **2** reveals the occurrence of an efficient TADF process showing that compound **2** exhibits excellent properties for harvesting all singlet and triplet excitons in the lowest excited singlet state in an emitter layer of an OLED (singlet harvesting).[37,48−51]

RESULTS AND DISCUSSION

In Figure 1, the structure of **2** is displayed as determined from X-ray investigations. The angle between the bipyridyl plane and

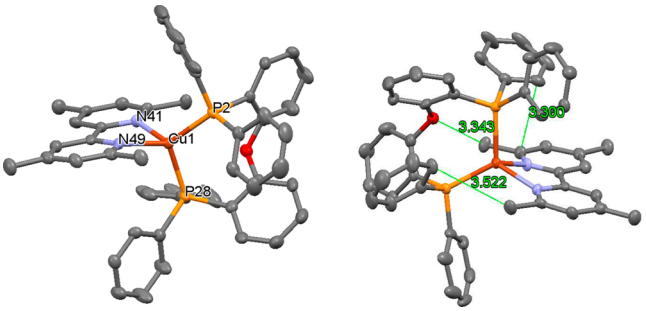

Figure 1. X-ray structure of **2** with probability ellipsoids set to 50% using the program Mercury.[89] Left: the tetrahedral coordination geometry around Cu. Right: short atom-to-atom contacts between the POP and the tmbpy ligands. H atoms are omitted for clarity.

the P−Cu−P plane of 81.95° shows limited flattening in the ground state away from an ideal 90°, and the chelating P−Cu−P angle is close to that of an ideal tetrahedron (Table 1), consistent with other Cu(POP) complexes reported by ourselves[85] and others.[53,86−88] The steric blocking that limits the flattening distortion upon excitation can be attributed to a combination of the POP and tmbpy ligands. The PCCOCCP chelating ring of the POP restricts the possible conformations of the phosphine ligands in comparison with two monodentate phosphines, and short interligand contacts are observed of 3.343 Å (C43−O21), 3.522 Å (C51−C10), and 3.300 Å (C40−C42; Figure 1). Significantly, the first two of these short contacts involve the 6,6′-methyl groups (Figure 1), demonstrating that these groups play an important role in limiting structural distortions.

First, discussion of the photophysical properties will focus on compound **2**. At ambient temperature, the powder, as received

Table 1. Selected Bond Lengths (Å) and Bond Angles (deg) from Single Crystal X-Ray Crystallography and Solvated (Ethanol Polarizable-Continuum Model) DFT Calculations for 2 and 1

	2		**2**	**1**
compound	X-ray		DFT	DFT
Cu−(N41)	2.089(3)	Cu−N	2.134	2.103
Cu−(N49)	2.097(3)		2.118	2.090
Cu−P(2)	2.2518(11)	Cu−P	2.477	2.426
Cu−P(28)	2.2901(11)		2.492	2.428
N(41)−Cu−N(49)	79.64(13)	N−Cu−N	79.99	80.01
N(41)−Cu−P(2)	121.85(9)		116.97	110.94
N(49)−Cu−P(2)	117.03(10)	N−Cu−P	114.27	118.69
N(41)−Cu−P(28)	103.50(10)		113.93	115.58
N(49)−Cu−P(28)	114.35(9)		117.98	114.82
P(2)−Cu−P(28)	115.25(4)		110.83	112.84

from the synthesis, exhibits yellow luminescence under excitation with UV light. The corresponding emission spectrum is broad and featureless, showing a peak at λ_{max} = 555 nm (Figure 2), and the emission decay time amounts to τ = 11 μs.

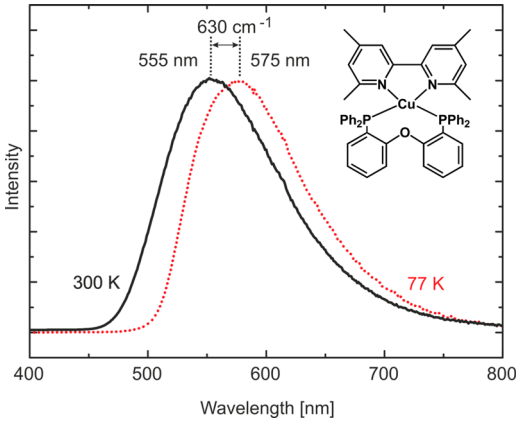

Figure 2. Emission spectra of compound [Cu(POP)(tmbpy)][BF_4] (**2**) (powder) recorded at temperatures of 300 and 77 K. The samples were excited at λ_{exc} = 350 nm.

Most notably, the compound's emission quantum yield is observed as Φ_{PL} = 55%. This places it among a relatively small number of highly emissive Cu(I) polypyridyl complexes reported in the literature.[80] Interestingly, the emission quantum yield can be further increased by grinding the substance between two glass plates. After this procedure, a quantum yield of Φ_{PL} = 74% is obtained for the ground powder. Also, a slight increase of the decay time to 13 μs is found. A comparison of the radiative $k_r = \Phi_{PL}\,\tau^{-1}$ and nonradiative $k_{nr} = (1 - \Phi_{PL})\,\tau^{-1}$ rates before and after grinding shows that the radiative rate is almost not affected by the grinding process, whereas the nonradiative rate is reduced by about a factor of 2 (Table 2). The emission spectra are not affected by grinding. The observed enhancement of the quantum yield could be caused by rearrangements in the solid material leading to a more rigid environment for the individual molecules.[84,90]

When compound **2** is dissolved in EtOH, the emission is red-shifted (λ_{max} = 575 nm) compared to the powder (λ_{max} = 555 nm). In addition, the quantum yield and the emission decay time decrease significantly in fluid EtOH solution (Φ_{PL}(powder) = 55%, Φ_{PL}(EtOH) = 6%, τ(powder) = 11 μs,

dx.doi.org/10.1021/ic500889s | Inorg. Chem. 2014, 53, 10854−10861

Table 2. Emission Data for Complexes 1 and 2 Recorded in Ethanol and Powder, Respectively

compound	[Cu(POP)(tmbpy)][BF$_4$] (**2**)	[Cu(POP)(dmbpy)][BF$_4$] (**1**)
EtOH		
λ_{max} (300 K) [nm]	575	655
τ (300 K) [μs]	2.5	0.02
ϕ_{PL} (300 K) [%]	6	<1
k_r (300 K) [s^{-1}]	2.4 × 10^4	
k_{nr} (300 K) [s^{-1}]	3.8 × 10^5	
λ_{max} (77 K) [nm]	535	605
τ (77 K) [μs]	73[a]	16[a]
powder		
λ_{max} (300 K) [nm]	555 (555)[b]	575
τ (300 K) [μs]	11 (13)[b]	--[c]
ϕ_{PL} (300 K) [%]	55 (74)[b]	9
k_r(300 K) [s^{-1}]	5.0 × 10^4 (5.7 × 10^4)[b]	
k_{nr}(300 K) [s^{-1}]	4.1 × 10^4 (2.0 × 10^4)[b]	
λ_{max} (77 K) [nm]	575	595
τ (77 K) [μs]	87	--[c]
ϕ_{PL} (77 K) [%]	47	
k_r (77 K) [s^{-1}]	5.3 × 10^3	
k_{nr} (77 K) [s^{-1}]	6.2 × 10^3	

[a]Slightly deviating from single-exponential decay. [b]Powder of compound **2** was measured as received from the reaction (and also after grinding between two glass plates). For compound **1**, no significant difference between ground and nonground powder was observed. [c]Strongly non-monoexponential decay.

τ(EtOH) = 2.5 μs). Such behavior has been reported for other Cu(I) compounds in the literature[37,49−51,54,65] and is attributed to the pronounced metal-to-ligand charge transfer (MLCT) character of the emitting state. In this excited state, the tendency of a geometry change toward planarization is strong in nonrigid environments. This leads to an energy stabilization (red-shift) and opens a highly effective nonradiative relaxation channel due to higher Franck−Condon factors of the excited and the ground state.[91] As a result, the quantum yield and emission decay time in fluid solution are drastically reduced. Cooling the solution to T = 77 K leads to a rigid cage around the complex through freezing of the solvent. This prevents distinct geometry changes upon excitation. As a consequence, the emission spectrum is blue-shifted and the decay time longer than the fluid situation.

Interestingly, compound **2** exhibits a significantly higher emission quantum yield (Φ_{PL} = 55/74%) than compound **1** (Φ_{PL} = 9%). This trend is also displayed in EtOH solution and can be attributed to the 6,6′-methyl groups present on the tmbpy ligand which act to sterically limit the flattening distortion consistent with the short atom-atom contacts observed (Figure 1). This effect is further discussed in more detail below.

For a more detailed understanding, the emission behavior of compound **2** (powder) was investigated at different temperatures (Figures 2 and 3). At T = 77 K, the emission decay time amounts to 87 μs and is therefore assigned to originate from the triplet state T_1 (while the ground state is a singlet S_0). With increasing temperature, the decay time decreases drastically to 11 μs at ambient temperature while the quantum yield does not change significantly between liquid nitrogen and ambient temperature (Φ_{PL}(300 K) = 55%, Φ_{PL}(77 K) = 47%). With this, the radiative rates can be calculated (k_r(300 K) = 5.0 × 10^4 s^{-1}, k_r(77 K) = 5.4 × 10^3 s^{-1}); i.e. a pronounced increase of the

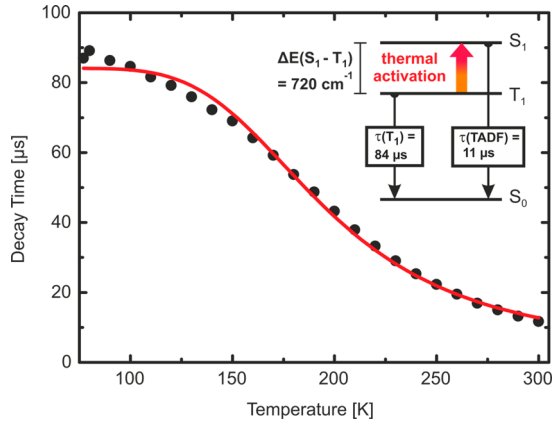

Figure 3. Emission decay time of compound **2** (powder) versus temperature. The decay times are closely monoexponential in the whole temperature range. The solid curve represents a fit according to eq 1. The parameters obtained from the fitting procedure amount to $\Delta E(S_1-T_1)$ = 720 cm^{-1}, $\tau(T_1)$ = 84 μs, and $\tau(S_1)$ = 160 ns.

radiative rates by almost a factor of 10 is observed on heating. This very strong increase is paralleled by a blue shift of the emission from 575 to 555 nm (peak to peak). Both effects, the increase of the radiative rate and the blue shift, can be rationalized by a thermal population of an energetically higher lying singlet state S_1 (Figure 3, inset). Accordingly, compound **2** clearly shows a thermally activated delayed fluorescence (TADF). The energy separation between the first excited singlet and triplet state $\Delta E(S_1-T_1)$ can be estimated from the shift of the emission spectra from 77 to 300 K, giving $\Delta E(S_1-T_1)$ = 630 cm^{-1} (Figure 2). An alternative approach to determine this energy separation results from the change of emission decay time as a function of temperature (Figure 3) according to eq 1.[48,51]

$$\tau(T) = \frac{3 + \exp\left[-\frac{\Delta E(S_1 - T_1)}{k_B T}\right]}{\frac{3}{\tau(T_1)} + \frac{1}{\tau(S_1)}\exp\left[-\frac{\Delta E(S_1 - T_1)}{k_B T}\right]} \quad (1)$$

In this equation, $\Delta E(S_1-T_1)$ represents the energy separation between the first excited singlet and triplet state, $\tau(S_1)$ and $\tau(T_1)$ are the emission decay times of the respective states, and k_B is the Boltzmann constant. From the fitting procedure, a value of $\Delta E(S_1-T_1)$ = 720 cm^{-1} results. Within limits of experimental error, this matches well the value obtained from the spectral shift. For the decay time of the first excited singlet state, a value of $\tau(S_1)$ = 160 ns was found. Such a value is in agreement with the singlet nature of this state, however, being connected with a relatively low oscillator strength of the $S_1 \leftrightarrow S_0$ transition. An emission originating as a prompt fluorescence was not found, presumably due to very fast intersystem crossing between S_1 and T_1. Moreover, the value found for $\tau(T_1)$ = 84 μs supports our assignment of a triplet state emission. We note that eq 1 can only be applied if the emitting states are in a thermal equilibrium. In the temperature range between 77 and 300 K, this condition is fulfilled.

Although the link between structural rigidity and high quantum yield is qualitatively well established, little detailed analysis has been directed toward more quantitative investigation for Cu(I) complexes.[43−52,60−62,66−76] Accordingly, to deepen our understanding of the effects of structural constraint and to direct future design of Cu(I) electroluminescent

dx.doi.org/10.1021/ic500889s | Inorg. Chem. 2014, 53, 10854−10861

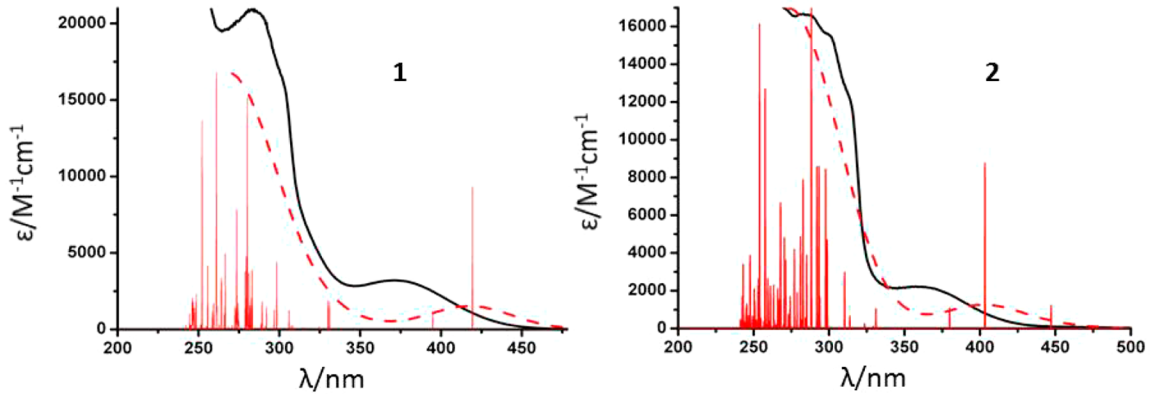

Figure 4. Theoretical UV/vis absorption spectra compared with experimental absorption spectra for **1** and **2**. Red vertical lines correspond to calculated electronic transisitons whereby the height refers to the calculated oscillator strength of the respective transition. Red dotted lines represent calculated spectra, and black solid lines represent the experimental spectra of **1** and **2** recorded in EtOH. The first 70 singlet transitions were calculated.

complexes, DFT geometry optimizations for the singlet ground state (Table 1, Figures S1 and S2, Tables S1 and S3) and triplet excited states of **1** and **2** were calculated using Gaussian 03[92] with the B3LYP/LANL2DZ[93−96] functional and basis set. This level of theory has been used successfully both in our previous work[85] and in the literature to calculate the structural and electronic properties of a number of coordination complexes.[83,53] The ground state singlet calculations for **1** and **2** were run with induced ethanol solvent effects to explore the ground state of the complex. The TDDFT calculations carried out on the optimized singlet ground state structure reproduce the experimental spectra reasonably well in the UV region, predicting a large number of transitions with significant oscillator strength (Figure 4, Tables S2 and S4). However, the calculated low-energy absorptions differ by around 2500 cm^{-1} from those seen experimentally, which is similar to some other literature calculations for charge-transfer transitions and can be attributed to the tendency of TDDFT calculations to underestimate the energies for this transition type.[83,97] The computational results allow insight into the orbital origins showing that the LUMO and LUMO+1 are bpy based and the HOMO to HOMO−3 are all Cu(I) or POP based,[85] confirming that the low energy transitions are Cu(I)/POP-to-bpy charge transfer in character.

Triplet excited state calculations have been used to investigate the excited state properties of the lowest triplet of **1** and **2**, both geometrically and electronically, to give insight into the connection between these properties within the systems. Due to computational difficulties, it was not possible to calculate an optimized geometry for the triplet states of either complex; hence a minimum energy structure was not obtained in the presence of the solvent effects, and instead a single-point solvent calculation was carried out. This procedure involves taking a computationally optimized structure executed without the presence of a solvent, and then applying a polarizable continuum model and recalculating the energy of the structure without optimizing the geometry. It was felt that this method could be applied to these structures as little variation in geometry was observed in the structures as solvents were introduced.

Triplet state computational studies were carried out using ArgusLab[98] input structures of **1** and **2**, and also starting from the crystal structure of **2**. The singlet ground state optimized geometries generated from the different starting structures for **2** revealed little difference between the energies of the structures, but there was a difference in the POP orientation, indicating its dependence upon the orientation of the input structure. This suggests the presence of multiple local minima in the energy profiles of these two complexes. Identification of which of these (if any) is the global minimum would require additional computational studies.

To explore the combination of POP and substituted bpys as geometry-constraining (hindering) ligands using DFT methods, we manipulated the geometries of **1** and **2** using the optimized singlet ground state geometries and also the X-ray structure of **2** as the starting point and calculated new overall complex energies of the optimized singlet and then single-point triplet excited states. This manipulation was carried out while fixing the torsion angle between the bpy and the POP ligands, as highlighted in Figure 5. For the ArgusLab input structures of

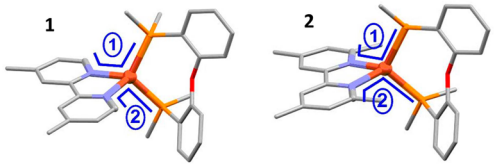

Figure 5. DFT geometry optimized singlet ground state structures of the cationic complexes **1** and **2**. The blue lines indicate the torsion angles that were manipulated. Using the Argus lab input structures, for both **1** and **2**, the torsion angles ① and ② were set to be equal. Using the crystal input structure for **2**, the torsion angles that correspond to ① and ② were not equal, and therefore we manipulated and quote the torsion angle ① C50−N49−Cu1−P28 (Table 3) = 80.63°. For comparison, the angle ② (C42−N41−Cu1−P2) in the crystal structure = 58.08°.

1 and **2**, both torsion angles were set to the same value; however, due to a nonsymmetrical starting geometry, the crystal structure input structure of **2** had the two torsion angles ① and ② set to different values (Table 3).

The torsion angle was varied by ±5° intervals starting from the optimized singlet geometry, and within this constraint, the optimized singlet and single-point triplet energies were then calculated. Figure 6 shows how the relative lowest-triplet energy of complexes **1** and **2** changes with a change of the torsion angle over a 30° range (Table 3). From this level of

dx.doi.org/10.1021/ic500889s | Inorg. Chem. 2014, 53, 10854−10861

Table 3. Selected Torsion Angle and Relative-Energy Data from the DFT Geometry Optimization of [Cu(POP)(dmbpy)]$^+$ (1) and [Cu(POP)(tmbpy)]$^+$ (2) Starting from the ArgusLab Input Structures, and for [Cu(POP)(tmbpy)]$^+$ (2) Starting from the Crystal Structure[a]

compound 1		compound 2		compound 2	
ArgusLab input		ArgusLab input		input from crystal structure	
torsion angle/deg	relative energy/kJmol^{-1}	torsion angle/deg	relative energy/kJmol^{-1}	torsion angle[e]/deg	relative energy/kJmol^{-1}
60	+7.21	55*		65*	
65	+3.77	60	+3.63	70	+3.78
70	+1.31	65	+0.56	75	+0.49
b	0	*c*	0	*d*	0
80	+0.43	75	+1.71	85	+0.77
85	+2.98	80	+4.96	90	+3.29
90	+7.19	85*		95*	

[a]All complexes are in their excited triplet states, without solvent corrections. For geometries labeled with an asterisk (*), a minimum energy structure was not achieved due to unacceptably short steric clashes. Energies are quoted relative to that of the structure before manipulation of the angle. [b]No manipulation: angles ①/② = 75.84°/75.43°. [c]No manipulation: angles ①/② = 69.91°/68.44°. [d]No manipulation. [e]Angle C50−N49−Cu1−P28 = 80.63°.

computational calculation it is not possible to state whether these structures are based around local or global minima. However, it was possible to calculate geometries for the manipulated structure of **1** over this entire 30° range. The curvature of the plots suggest a similarity in the flexibility of the two complexes only within ±10° of the optimized torsion angle, with roughly the same small energy increase with each 5° manipulation of the bpy ligand for both **1** and **2**.

Once the torsion angle was increased by ±15° (Table 3), optimization of **2** led to unacceptably high energies as these manipulated structures place the 6,6′-methyl groups in too close a proximity to the phenyls of the POP ligand (Figure 7). Triplet geometry calculations starting from the crystal structure of **2** indicate that although the geometries differ from the ArgusLab input structure, they exhibit largely similar overall complex energies and structural behavior (Table 3, Figure S3).

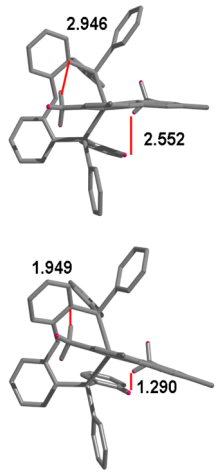

Figure 7. DFT geometry optimization of [Cu(POP)(tmbpy)]$^+$ (**2**) starting from the ArgusLab inputted structures with torsion angles of 60° (upper) and 55° (lower), showing unacceptable steric clashes for the latter in comparison with the former. (Sum of Van der Waals radii H···H = 2.40 Å; C···H = 3.05 Å.[99]) Distances are shown in Ångstroms. For clarity, a stick model, with irrelevant H atoms omitted, has been used.

CONCLUSION

In this contribution, we demonstrate how slight modification of the chemical structure of a [Cu^{I}(diimine)(diphosphine)]$^+$ complex can lead to a substantial increase of the emission quantum yield. In the case of the [Cu(POP)(dmbpy)]$^+$ complex, this is achieved by the increase of the steric demand of the bipyridine ligand through the introduction of two additional methyl groups resulting in the [Cu(POP)(tmbpy)]$^+$ complex. In combination with the bulky POP ligand, these groups limit the photoinduced flattening distortion that the compound can undergo on excitation of an MLCT state. As a result, the nonradiative deactivation to the ground state is significantly reduced, leading to around a 6-fold increase of the emission quantum yield from 9 to 55% (or even 74% for the sample after grinding).

These observations demonstrate the increased rigidity enforced upon the structure of **2** compared to that present in **1** as a result of the steric demands of the 6,6′-methyl groups on the bipyridyl ligands. The attempt to calculate structures for **2**

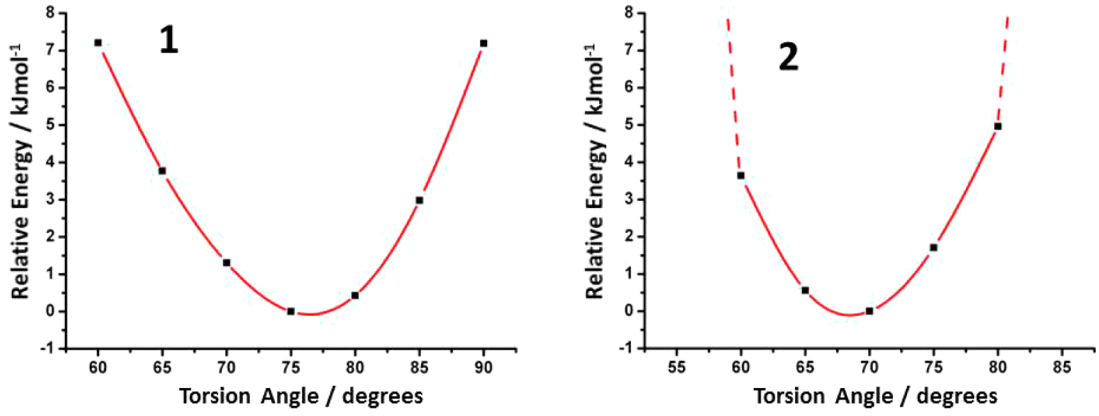

Figure 6. Plots of DFT calculated relative single-point triplet energies for **1** and **2** against the torsion angle, starting from ArgusLab input structures. Note that *y* axes are the same scale and *x* axes are the same range and scale, and that the curve is there to act as a guide to the eye. For **2**, the dashed red lines represent the unacceptably high energies calculated at a larger angle, due to clashing hydrogen atoms.

dx.doi.org/10.1021/ic500889s | Inorg. Chem. 2014, 53, 10854−10861

where the torsion angle between the two ligands has been manipulated to 55° shows the unacceptably short H···H distance of 1.290 Å, (c.f. the sum of the H···H Van der Waal radii of 2.40 Å[99]) between an H-atom on a peripheral ring of the POP and an H-atom on a methyl group in the 6 position of the bipy. This clearly illustrates the inability of the pseudotetrahedral structure of **2** to flatten beyond a threshold value of around ±10°. In contrast, compound **1** can further flatten with only an incremental additional energy penalty. Significantly, the flexibility of **1** and **2** seems little different within the limited geometric range ±10°, and these observations are reminiscent of the concept of a "steric threshold" introduced in other areas of chemistry,[100] whereby the abrupt onset of steric effects occurs beyond some geometric limit, before which steric effects play a negligible role. Although it is not possible to generalize to all Cu(I) complexes, our observations suggest a shallow potential well with unconstrained structural flexibility up to a certain range before an abrupt limit to the distortion.

Most interestingly, for the sterically constrained compound **2**, it was found that at ambient temperature the emission is largely determined by a thermally activated delayed fluorescence (TADF). At ambient temperature, the compound emits almost only from the first excited singlet state S_1 (^{1}MLCT) which is thermally populated from the T_1 state (^{3}MLCT). This results in a relatively short emission decay time of 11 μs at ambient temperature as compared to the triplet state decay time of $\tau(T_1)$ = 84 μs.

Recently, it has been demonstrated that emitters exhibiting a TADF are very attractive for application in electroluminescent devices, such as OLEDs, as they can make use of the singlet harvesting effect.[37,48−51,101] Cu(I) complexes, such as compound **2** ($[Cu(POP)(tmbpy)]^+$), are attractive candidates in this regard. However, also purely organic molecules have recently been demonstrated to exhibit an efficient TADF at ambient temperatures and might be an interesting alternative to transition-metal compounds.[102,103] Which of the two concepts will be superior for future applications is not yet clear. The lowest triplet state of organic TADF molecules experiences very weak SOC, and thus, intersystem crossing (ISC) is relatively slow. Besides the size of the energy gap $\Delta E(S_1-T_1)$, this seems to be a limiting factor for the TADF decay time. Thus, it might become too long and result in saturation effects in OLEDs giving an undesired roll-off of the efficiency with increasing current density. On the other hand, SOC in Cu(I) complexes is usually high enough to induce fast ISC. As a consequence, the TADF decay time is essentially determined by the energy gap $\Delta E(S_1-T_1)$ and, slightly less importantly, by the allowance of the S_0-S_1 transition.

EXPERIMENTAL SECTION

Complexes **1** and **2** were prepared as reported previously.[85] The steady-state emission spectroscopy was carried out with **1** and **2** dissolved in ethanol at concentrations of about 10^{-5} mol dm^{-3}. Fluid solutions were degassed by at least five pump−freeze−thaw cycles with a final vapor pressure at 77 K of ~10^{-5} mbar, while the powder samples were measured under a nitrogen atmosphere.

The absorption spectra were recorded with a Perkin-Elmer Lambda 9 spectrophotometer controlled by the UV/Winlab software. Emission spectra at all temperatures were measured with a steady-state fluorescence spectrometer (Jobin Yvon Fluorolog 3). Luminescence quantum yields at ambient temperature and 77 K were determined with an integrating sphere (Hamamatsu Photonics, C9920-02), which exhibits a highly reflective Spectralon inside coating. The relative error of the measured values is ±0.10. Temperature dependent measurements were carried out in a helium cryostat (Cryovac Konti Cryostat IT) in which helium gas flow and pressure as well as heating were controlled. Excited state decay curves were recorded using a diode laser (Picobrite PB-375L) with a wavelength of 378 nm and a pulse width < 100 ps as excitation source.

Crystals were grown by slow diffusion of hexane into an acetone solution of **2**. Single crystal X-ray diffraction data were collected using Mo Kα radiation (λ = 0.71073 Å) on a Smart APEX CCD diffractometer equipped with an Oxford Cryosystems low-temperature device operating at 150 K. An absorption correction was applied by the multiscan procedure SADABS.[104] The structures were solved by direct methods (Shelx)[105] and refined by full-matrix least-squares against F using all data (Shelx).[105] The SQUEEZE routine within PLATON was used to treat disorder of the included solvent and counterion, with one molecule of hexane and one BF_4^- anion per formula unit removed from the cell.[106] Figures were prepared with the program Mercury.[89] All non-H atoms were refined with anisotropic displacement parameters. X-ray crystallography of **2**: $C_{50}H_{44}CuN_2OP_2{\cdot}BF_4{\cdot}C_6H_{14}$, MW = 987.39, T/K = 100(2), triclinic $P\bar{1}$, a = 11.35159(16), b = 12.3287(2), c = 17.7320(3) Å, α = 70.8270(17), β = 80.0951(13), γ = 77.4948(14)°, V = 2274.59(7) Å^3, Z = 2, D_{calcd}/M g m^{-3} = 1.44, independent reflections = 8960 [R_{int} = 0.049], data/restraints/parameters = 8960/0/505, absorption correction = 1.845 mm^{-1}, R_1/wR (observed data: $F^2 > 2\sigma(F^2)$) = 0.0937/0.0810, CCDC 989087.

Density functional theory calculations were performed using the Gaussian 03 program[92] with the starting structures for **1** and **2** input through the builder program ArgusLab and/or the crystal structure coordinates where appropriate. All calculations were carried out using Becke's three parameter exchange functional with the Lee−Yang−Parr for the correlation functional (B3LYP),[96] and the Los Alamos National Laboratory basis sets, known as LANL2DZ (developed by Hay and Wadt),[93−95] which comprises effective core potential (ECP) + double-ζ for copper, and the all-electron valence double-ζ basis sets developed by Dunning (D95V) for light atoms.[107] Vibrational frequency calculations were carried out to ensure that optimized geometries were minima on the potential energy surface. Solvent effects were included via the self-consistent reaction field (SCRF) method using the polarized continuum model (PCM),[108] with slight modifications to the default cavity parameters to aid convergence. Time-dependent density functional theory (TDDFT) calculations were performed in an ethanol polarizable continuum model, with the first 70 singlet transitions calculated. Starting structures for the singlet and triplet states of **1** and **2** were input through the builder program ArgusLab.

ASSOCIATED CONTENT

Supporting Information

Results of DFT and TDDFT calculations. This material is available free of charge via the Internet at http://pubs.acs.org.

AUTHOR INFORMATION

Corresponding Authors

*Tel.: +49 941 943 4464. Fax: +49 941 943 4488. E-mail: hartmut.yersin@ur.de.

*Tel.: +44 131 650 4755. Fax: +44 131 650 4742. E-mail: neil.robertson@ed.ac.uk

Notes

The authors declare no competing financial interest.

ACKNOWLEDGMENTS

We thank EPSRC and EaStChem for funding, including the EaStChem Research Computing Facility (http://www.eastchem.ac.uk/rcf). This facility is partially supported by the eDIKT initiative (heep://www.edikt.org). We also gratefully acknowledge funding by the German Ministry of Education and Research (BMBF).

REFERENCES

(1) Yersin, H. *Highly Efficient OLEDs with Phosphorescent Materials*; Wiley-VCH: Weinheim, Germany, 2008.
(2) Brütting, W.; Adachi, C. *Physics of Organic Semiconductors*; Wiley-VCH: Weinheim, Germany, 2012.
(3) Gao, F. G.; Bard, A. J. *J. Am. Chem. Soc.* **2000**, *122*, 7426−7427.
(4) Kim, S. Y.; Baik, J. M.; Yu, H. K.; Lee, J-L. *J. Appl. Phys.* **2005**, *98*, 093707−093707.
(5) Cheng, G.; Chow, P-K.; Kui, S. C. F.; Kwok, C-C.; Che, C-M. *Adv. Mater.* **2013**, *25*, 6765−6770.
(6) Xiao, L.; Chen, Z.; Qu, B.; Luo, J.; Kong, S.; Gong, G.; Kido, J. *Adv. Mater.* **2011**, *23*, 926−952.
(7) Pei, Q.; Yu, G.; Zhang, C.; Yang, Y.; Heeger, A. J. *Science* **1995**, *269*, 1086−1088.
(8) Pei, Q.; Yang, Y; Yu, G.; Zhang, C; Heeger, A. J. *J. Am. Chem. Soc.* **1996**, *118*, 3922−3929.
(9) Slinker, J. D.; DeFranco, J. A.; Jaquith, M. J.; Silveira, W. R.; Zhong, Y-W.; Moran-Mirabal, J. M.; Craighead, H. G.; Abruna, H. D.; Marohn, J. A.; Malliaras, G. G. *Nat. Mater.* **2007**, *6*, 894−899.
(10) Wang, X-D.; Wolfbeis, O. S.; Meier, R. J. *Chem. Soc. Rev.* **2013**, *42*, 7834−7869.
(11) Karakus, C.; Fischer, L. H.; Schmeding, S.; Hummel, J.; Risch, N.; Schäferling, M.; Holder, E. *Dalton Trans* **2012**, *41*, 9623.
(12) Mak, C. S. K.; Pentlehner, D.; Stich, M.; Wolfbeis, O. S.; Chan, W. K.; Yersin, H. *Chem. Mater.* **2009**, *21*, 2173−2175.
(13) O'Regan, B.; Grätzel, M. *Nature* **1991**, *353*, 737−740.
(14) Nazeeruddin, M. K. *Coord. Chem. Rev.* **2004**, *248*, 1161−1164.
(15) Robertson, N. *ChemSusChem* **2008**, *1*, 977−979.
(16) Alonso-Vante, N.; Nierengarten, J.-F.; Sauvage, J.-P. *J. Chem. Soc., Dalton Trans.* **1994**, 1649−1654.
(17) Sakaki, S.; Kuroki, T.; Hamada, T. *J. Chem. Soc., Dalton Trans.* **2002**, 840−842.
(18) Bessho, T.; Constable, E. C.; Graetzel, M.; Redondo, A. H.; Housecroft, C. E.; Kylberg, W.; Nazeeruddin, M. K.; Neuburger, M.; Schaffner, S. *Chem. Commun.* **2008**, 3717−3719.
(19) Constable, E. C.; Redondo, A. H.; Housecroft, C. E.; Neuburger, M.; Schaffner, S. *Dalton Trans.* **2009**, *39*, 6634−6644.
(20) Bozic-Weber, B.; Constable, E. C.; Housecroft, C. E.; Neuburger, M.; Price, J. R. *Dalton Trans.* **2010**, *39*, 3585−3594.
(21) Bozic-Weber, B.; Constable, E. C.; Housecroft, C. E.; Kopecky, P.; Neuburger, M.; Zampese, J. A. *Dalton Trans.* **2011**, *40*, 12584−12594.
(22) Bozic-Weber, B.; Chaurin, V.; Constable, E. C.; Housecroft, C. E.; Meuwly, M.; Neuburger, M.; Rudd, J. A.; Schönhofer, E.; Siegfried, L. *Dalton Trans.* **2012**, *41*, 14157−14169.
(23) Yuan, Y-J.; Yu, Z-T.; Zhang, J-Y.; Zou, Z-G. *Dalton Trans.* **2012**, *41*, 9594−9597.
(24) Bozic-Weber, B.; Brauchli, S. J.; Constable, E. C.; Fürer, S. O.; Housecroft, C. E.; Malzner, F. J.; Wright, I. A.; Zampese, J. A. *Dalton Trans.* **2013**, *42*, 12293.
(25) Sandroni, M.; Kayanuma, M.; Planchat, A.; Szuwarski, N.; Blart, E.; Pellegrin, Y.; Daniel, C.; Boujtita, M.; Odobel, F. *Dalton Trans.* **2013**, *42*, 10818.
(26) Bozic-Weber, B.; Constable, E. C.; Housecroft, C. E. *Coord. Chem. Rev.* **2013**, *257*, 3089.
(27) Hewat, T. E.; Yellowlees, L. J.; Robertson, N. *Dalton Trans.* **2014**, *43*, 4127.
(28) Vos, J. G.; Kelly, J. M. *Dalton Trans.* **2006**, *36*, 4869−4883.
(29) Nazeeruddin, M. K.; Kay, A.; Rodicio, I.; Humphry-Baker, R.; Mueller, E.; Liska, P.; Vlachopoulos, N.; Grätzel, M. *J. Am. Chem. Soc.* **1993**, *115*, 6382−6390.
(30) Meyer, T. *Pure, Appl. Chem.* **1986**, *58*, 1193−1206.
(31) Juris, A.; Balzani, V.; Barigelletti, F.; Campagna, S.; Belser, P.; von Zelewsky, A. *Coord. Chem. Rev.* **1988**, *84*, 85−277.
(32) Yersin, H.; Humbs, W.; Strasser, J. *Coord. Chem. Rev.* **1997**, *159*, 325.
(33) Michael, S. L.; Stefan, B. *Chem.—Eur. J.* **2006**, *12*, 7970−7977.
(34) Chou, P-T.; Chi, Y. *Chem.—Eur. J.* **2007**, *13*, 380−395.
(35) Hofbeck, T.; Yersin, H. *Inorg. Chem.* **2010**, *49*, 9290−9299.
(36) Rausch, A. F.; Thompson, M. E.; Yersin, H. *J. Phys. Chem. A* **2009**, *113*, 5927−5932.
(37) Yersin, H.; Rausch, A. F.; Czerwieniec, R.; Hofbeck, T.; Fischer, T. *Coord. Chem. Rev.* **2011**, *255*, 2622−2652.
(38) Williams, J. A. G. *Top. Curr. Chem.* **2007**, *281*, 205−268.
(39) Che, C-M.; Kwok, C-C.; Lai, S-W.; Rausch, A. F.; Finkenzeller, W. J.; Zhu, N.; Yersin, H. *Chem.—Eur. J.* **2010**, *16*, 233−247.
(40) Williams, J. A. G.; Develay, S.; Rochester, D. L.; Murphy, L. *Coord. Chem. Rev.* **2008**, *252*, 2596−2611.
(41) Bossi, A.; Rausch, A. F.; Leitl, M. J.; Czerwieniec, R.; Whited, M. T.; Djurovich, P. I.; Yersin, H.; Thompson, M. E. *Inorg. Chem.* **2013**, *52*, 12403−12415.
(42) Culham, S.; Lanoë, P-H.; Whittle, V. L.; Durrant, M. C.; Williams, J. A. G.; Kozhevnikov, V. N. *Inorg. Chem.* **2013**, *52*, 10992−11003.
(43) Blaskie, M. W.; McMillin, D. R. *Inorg. Chem.* **1980**, *19*, 3519−3522.
(44) Palmer, C. E. A.; McMillin, D. R. *Inorg. Chem.* **1987**, *26*, 3837−3840.
(45) Kirchhoff, J. R.; McMillin, D. R.; Robinson, W. R.; Powell, D. R.; McKenzie, A. T.; Chen, S. *Inorg. Chem.* **1985**, *24*, 3928−3933.
(46) Blasse, G.; McMillin, D. R. *Chem. Phys. Lett.* **1980**, *70*, 1−3.
(47) Gushurst, A. K. I.; McMillin, D. R.; Dietrich-Buchecker, C. O.; Sauvage, J. P. *Inorg. Chem.* **1989**, *28*, 4070−4072.
(48) Leitl, M. J.; Küchle, F. R.; Mayer, H. A.; Wesemann, L.; Yersin, H. *J. Phys. Chem. A* **2013**, *117*, 11823−11836.
(49) Czerwieniec, R.; Yu, J.; Yersin, H. *Inorg. Chem.* **2011**, *50*, 8293−8301.
(50) Zink, D. M.; Bächle, M.; Baumann, T.; Nieger, M.; Kuhn, M.; Wang, C.; Klopper, W.; Monkowius, U.; Hofbeck, T.; Yersin, H.; Bräse, S. *Inorg. Chem.* **2013**, *52*, 2292−305.
(51) Czerwieniec, R.; Kowalski, K.; Yersin, H. *Dalton Trans.* **2013**, *42*, 9826.
(52) Armaroli, N. *Chem. Soc. Rev.* **2001**, *30*, 113−124.
(53) Costa, R. D.; Tordera, D.; Orti, E.; Bolink, H. J.; Schönle, J.; Graber, S.; Housecroft, C. E.; Constable, E. C.; Zampese, J. A. *J. Mater. Chem.* **2011**, *21*, 16108.
(54) Tsuboyama, A.; Kuge, K.; Furugori, M.; Okada, S.; Hoshino, M.; Ueno, K. *Inorg. Chem.* **2007**, *46*, 1992−2001.
(55) Igawa, S.; Hashimoto, M.; Kawata, I.; Yashima, M.; Hoshino, M.; Osawa, M. *J. Mater. Chem. C* **2013**, *1*, 542−551.
(56) Deaton, J. C.; Switalski, S. C.; Kondakov, D. Y.; Young, R. H.; Pawlik, T. D.; Giesen, D. J.; Harkins, S. B.; Miller, A. J. M.; Mickenberg, S. F.; Peters, J. C. *J. Am. Chem. Soc.* **2010**, *132*, 9499−9508.
(57) Osawa, M. *Chem. Commun.* **2014**, *50*, 1801−1803.
(58) Krylova, V. A.; Djurovich, P. I.; Aronson, J. W.; Haiges, R.; Whited, M. T.; Thompson, M. E. *Organometallics* **2012**, *31*, 7983−7993.
(59) Krylova, V. A.; Djurovich, P. I.; Whited, M. T.; Thompson, M. E. *Chem. Commun.* **2010**, *46*, 6696−6698.
(60) Miller, A. J. M.; Dempsey, J. L.; Peters, J. C. *Inorg. Chem.* **2007**, *46*, 7244−7246.
(61) Armaroli, N.; Accorsi, G.; Cardinali, F.; Listorti, A. *Top. Curr. Chem.* **2007**, *280*, 69−115.
(62) Everly, R. M.; McMillin, D. R. *J. Phys. Chem.* **1991**, *95*, 9071−9075.
(63) Vorontsov, I. I.; Graber, T.; Kovalevsky, A. Y.; Novozhilova, I. V.; Gembicky, M.; Chen, Y.-S.; Coppens, P. *J. Am. Chem. Soc.* **2009**, *131*, 6566−6573.
(64) Coppens, P.; Sokolow, J.; Trzop, E.; Makal, A.; Chen, Y. *J. Phys. Chem. Lett.* **2013**, *4*, 579−582.
(65) Yersin, H.; Rausch, A. F.; Czerwieniec, R. *Physics of Organic Semiconductors*; Wiley-VCH: Weinheim, Germany, 2012; p 371.
(66) Williams, R. M.; De Cola, L.; Hartl, F.; Lagref, J-F.; Planeix, J-M.; Cian, A. D.; Hosseini, M. W. *Coord. Chem. Rev.* **2002**, *230*, 253−261.
(67) Pallenberg, A. J.; Koenig, K. S.; Barnhart, D. M. *Inorg. Chem.* **1995**, *34*, 2833−2840.

(68) Ruthkosky, M.; Kelly, C. A.; Castellano, F. N.; Meyer, G. J. *Coord. Chem. Rev.* **1998**, *171*, 309−322.
(69) Miller, M. T.; Gantzel, P. K.; Karpishin, T. B. *Inorg. Chem.* **1998**, *37*, 2285−2290.
(70) Miller, M. T.; Gantzel, P. K.; Karpishin, T. B. *Inorg. Chem.* **1999**, *38*, 3414−3422.
(71) Siddique, Z. A.; Yamamoto, Y.; Ohno, T.; Nozaki, K. *Inorg. Chem.* **2003**, *42*, 6366−6378.
(72) Iwamura, M.; Takeuchi, S.; Tahara, T. *J. Am. Chem. Soc.* **2007**, *129*, 5248−5256.
(73) Leydet, Y.; Bassani, D. M.; Jonusauskas, G.; McClenaghan, N. D. *J. Am. Chem. Soc.* **2007**, *129*, 8688−8689.
(74) Green, O.; Gandhi, B. A.; Burstyn, J. N. *Inorg. Chem.* **2009**, *48*, 5704−5714.
(75) Che, G.; Su, Z.; Li, W.; Chu, B.; Li, M.; Hu, Z.; Zhang, Z. *Appl. Phys. Lett.* **2006**, *89*, 103511−103513.
(76) Andrés-Tomé, I.; Fyson, J.; Baiao Dias, F.; Monkman, A. P.; Iacobellis, G.; Coppo, P. *Dalton Trans.* **2012**, *41*, 8669.
(77) Cuttell, D. G.; Kuang, S-M.; Fanwick, P. E.; McMillin, D. R.; Walton, R. A. *J. Am. Chem. Soc.* **2001**, *124*, 6−7.
(78) Kuang, S-M.; Cuttell, D. G.; McMillin, D. R.; Fanwick, P. E.; Walton, R. A. *Inorg. Chem.* **2002**, *41*, 3313−3322.
(79) Zhang, Q.; Zhou, Q.; Cheng, Y.; Wang, L.; Ma, D.; Jing, X.; Wang, F. *Adv. Mater.* **2004**, *16*, 432−436.
(80) Armaroli, N.; Accorsi, G.; Holler, M.; Moudam, O.; Nierengarten, J. F.; Zhou, Z.; Wegh, R. T.; Welter, R. *Adv. Mater.* **2006**, *18*, 1313−1316.
(81) Armaroli, N.; Accorsi, G.; Bergamini, G.; Ceroni, P.; Holler, M.; Moudam, O.; Duhayon, C.; Delavaux-Nicot, B.; Nierengarten, J. F. *Inorg. Chim. Acta* **2007**, *360*, 1032−1042.
(82) Xia, H.; He, L.; Zhang, M.; Zeng, M.; Wang, X.; Lu, D.; Ma, Y. *Opt. Mater.* **2007**, *29*, 667−671.
(83) Yang, L.; Feng, J-K.; Ren, A-M.; Zhang, M.; Ma, Y-G.; Liu, X-D. *Eur. J. Inorg. Chem.* **2005**, 1867−1879.
(84) Zhang, L.; Li, B.; Su, Z. *Langmuir* **2009**, *25*, 2068−2074.
(85) Linfoot, C. L.; Richardson, P.; Hewat, T. E.; Moudam, O.; Forde, M. M.; Collins, A.; White, F.; Robertson, N. *Dalton Trans.* **2010**, *39*, 8945.
(86) McCormick, T.; Jia, W-L.; Wang, S. *Inorg. Chem.* **2005**, *45*, 147−155.
(87) Moudam, O.; Kaeser, A.; Delavaux-Nicot, B.; Duhayon, C.; Holler, M.; Accorsi, G.; Armaroli, N.; Séguy, I.; Navarro, J.; Destruel, P.; Nierengarten, J. F. *Chem. Commun.* **2007**, 3077.
(88) Sun, W.; Zhang, Q.; Qin, L.; Cheng, Y.; Xie, Z.; Lu, C.; Wang, L. *Eur. J. Inorg. Chem.* **2010**, 4009−4017.
(89) Macrae, C. F.; Edgington, P. R.; McCabe, P.; Pidcock, E.; Shields, G. P.; Taylor, R.; Towler, M.; van de Streek, J. *J. Appl. Crystallogr.* **2006**, *39*, 453−457.
(90) Volz, D.; Nieger, M.; Friedrichs, J.; Baumann, T.; Brase, S. *Langmuir* **2013**, *29*, 3034−44.
(91) Turro, N. J. *Modern Molecular Chemistry*; Benjamin/Cummings Publishing Company, Inc.: Menlo Park, CA, 1978.
(92) Frisch, M. J.; Trucks, G. W.; Schlegel, H. B.; Scuseria, G. E.; Robb, M. A.; Cheeseman, J. R.; Montgomery, J. A.; Vreven, J. T.; Kudin, K. N.; Burant, J. C.; Millam, J. M.; Iyengar, S. S.; Tomasi, J.; Barone, V.; Mennucci, B; Cossi, M.; Scalmani, G.; Rega, N.; Petersson, G. A.; Nakatsuji, H.; Hada, M.; Ehara, M.; Toyota, K.; Fukuda, R.; Hasegawa, J.; Ishida, M.; Nakajima, T.; Honda, Y.; Kitao, O.; Nakai, H.; Klene, M.; Li, X.; Knox, J. E.; Hratchian, H. P.; Cross, J. B.; Bakken, V.; Adamo, C.; Jaramillo, J.; Gomperts, R.; Stratmann, R. E.; Yazyev, O.; Austin, A. J.; Cammi, R.; Pomelli, C.; Ochterski, J. W.; Ayala, P. Y.; Morokuma, K.; Voth, G. A.; Salvador, P.; Dannenberg, J. J.; Zakrzewski, V. G.; Dapprich, S.; Daniels, A. D.; Strain, M. C.; Farkas, O.; Malick, D. K.; Rabuck, A. D.; Raghavachari, K.; Foresman, J. B.; Ortiz, J. V.; Cui, Q.; Baboul, A. G.; Clifford, S.; Cioslowski, J.; Stefanov, B. B.; Liu, G.; Liashenko, A.; Piskorz, P.; Komaromi, I.; Martin, R. L.; Fox, D. J.; Keith, T.; Al-Laham, M. A.; Peng, C. Y.; Nanayakkara, A.; Challacombe, M.; Gill, P. M. W.; Johnson, B.; Chen, W.; Wong, M. W.; Gonzalez, C.; Pople, J. A. *Gaussian 03*, revision E.01; Gaussian, Inc.: Wallingford, CT, 2004.
(93) Wadt, W. R.; Hay, P. J. *J. Chem. Phys.* **1985**, *82*, 284−298.
(94) Wadt, W. R.; Hay, P. J. *J. Chem. Phys.* **1985**, *82*, 270−283.
(95) Wadt, W. R.; Hay, P. J. *J. Chem. Phys.* **1985**, *82*, 299−310.
(96) Becke, A. D. *J. Chem. Phys.* **1993**, *98*, 5648−5652.
(97) McCall, K. L.; Jennings, J. R.; Wang, H.; Morandeira, A.; Peter, L. M.; Durrant, J. R.; Yellowlees, L. J.; Woollins, J. D.; Robertson, N. *J. Photochem. Photobiol., A* **2009**, *202*, 196−204.
(98) Thompson, M. A. http://www.arguslab.com.
(99) *Inorganic Chemistry*, 4th edition; Housecroft, C. E., Sharpe, A. G., Eds.; Pearson Education Limited: England, 2012
(100) Brown, T. L.; Lee, K. J. *Coord. Chem. Rev.* **1993**, *128*, 89.
(101) Zink, D. M.; Volz, D.; Baumann, T.; Mydlak, M.; Flügge, H.; Friedrichs, J.; Nieger, M.; Bräse, S. *Chem. Mater.* **2013**, *25*, 4471−4486.
(102) Zhang, Q. S.; Li, B.; Huang, S. P.; Nomura, H.; Tanaka, H.; Adachi, C. *Nat. Photonics* **2014**, *8*, 326−332.
(103) Uoyama, H.; Goushi, K.; Shizu, K.; Nomura, H.; Adachi, C. *Nature* **2012**, *492*, 234−238.
(104) Sheldrick, G. M. *SADABS*; University of Gottingen: Gottingen, Germany.
(105) Sheldrick, G. *Acta Crystallogr., Sect. A* **2008**, *64*, 112−122.
(106) Spek, A. *J. Appl. Crystallogr.* **2003**, *36*, 7−13. van der Sluis, P; Spek, A. L. *Acta Crystallogr.* **1990**, *A46*, 194−201.
(107) Dunning, T. H.; Schaefer, H. F.; Hay, P. J. *Modern Theoretical Chemisrty, Ed III*; Plenum: New York, 1976.
(108) Vleck, A., Jr.; Zális, S. *Coord. Chem. Rev.* **2007**, *251*, 258−287.